

Carbon-Catalyzed Oxidative Dehydrogenation of *n*-Butane: Selective Site Formation during sp^3 -to- sp^2 Lattice Rearrangement**

Xi Liu, Benjamin Frank, Wei Zhang, Thomas P. Cotter, Robert Schlögl, and Dang Sheng Su*

Research on sp^3 - and sp^2 -hybridized nanostructured carbon materials has stimulated a vital interest from academia and industry.^[1] Nanocarbons and carbon-based composites such as C_3N_4 provide a great potential as metal-free catalysts, for example for C–H bond activation, C=C bond hydrogenation, or water splitting.^[2–4] The chemical nature of the carbon surface is tuneable over a wide range by its defect density and decoration with various types of heteroatom functionalities.^[5–7] Low-dimensional nanocarbons with a well-defined microstructure have remarkable stability and coke-resistance in the catalytic hydrocarbon oxidation and oxidative dehydrogenation (ODH). Studies on the reaction mechanism suggest that surface quinoidic groups mimic the lattice oxygen atoms of metal oxide catalysts and play the key role for dehydrogenation of the hydrocarbon molecule,^[8] whereas the subsurface bulk serves as skeleton and is hardly influenced by the surface activation.^[2] However, it has generally been ignored that carbon nanotubes (CNT) as graphitic materials are thermodynamically stable and thus an impact of the surface reaction on sublayer atoms could hardly be identified by any technique. A correlation between structural sensitivity and catalytic performance has been observed in the case of butane oxidation, wherein a chemically induced phase transition of $VOPO_4$ occurs.^[9] Therefore, a discrete and in-depth analysis of the combination of the kinetically controlled ODH reaction and the thermodynamically controlled surface-activation process, that is, the change in surface and bulk properties of the catalyst under reaction conditions, can provide new insights into material dynamics on the nanometer scale.

Herein we report on the superior catalytic performance of ultradispersed diamonds (UDD; Beijing Grish Hitech Co., China) for the ODH of *n*-butane to butenes. The material was

obtained by an explosion method and isolated from the detonation soot by oxidative treatment with H_2SO_4 and $HClO_4$ acids.^[10,11] The high surface area of UDD ($320\text{ m}^2\text{ g}^{-1}$) allows for an observable catalytic turnover comparable to CNT catalysts. Catalysis induces a comprehensive carbon lattice rearrangement from cubic sp^3 -hybridized UDD to graphitic sp^2 -hybridized supramolecular fullerene shells, while preserving the high surface area of $328\text{ m}^2\text{ g}^{-1}$ after the catalytic tests. This structural transformation brings up a carbon surface that acts highly selective in the ODH of *n*-butane. UDD is thermodynamically unstable and the phase transition from UDD to onionlike carbon (OLC) attracts attention because of its high potential as an electromagnetic radiation-shielding material.^[12] In general, the graphitization is kinetically hindered and requires extreme reaction conditions ($T > 1000\text{ K}$, inert atmosphere). Thus, the surface-induced lattice rearrangement provides intuitive and convincing evidence for a surface-activation process of the UDD catalyst.

A comparison of the catalytic performance of different nanocarbons is shown in Figure 1a and Table 1. Similar conversions in the range of 9–12% allow for direct comparison of selectivities regardless of the Wheeler type III reaction

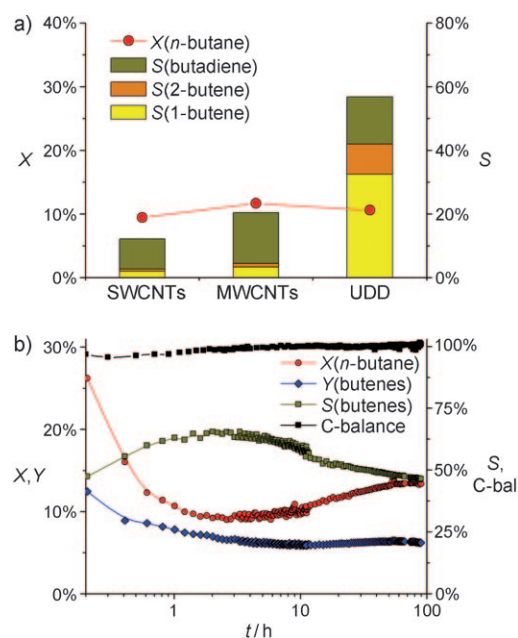


Figure 1. a) Catalytic performance of various nanocarbons after 10 h time-on-stream, X = conversion, S = selectivity; b) evolution of the catalytic performance of UDD, X = conversion, Y = yield, S = selectivity, C-bal = carbon balance.

[*] Dr. X. Liu, Dr. B. Frank, Dr. W. Zhang, T. P. Cotter, Prof. R. Schlögl, Prof. Dr. D. S. Su

Department of Inorganic Chemistry
Fritz Haber Institute of the Max Planck Society
Faradayweg 4–6, 14195 Berlin (Germany)
Fax: (+49) 30-8413-4401
E-mail: dangsheng@fhi-berlin.mpg.de

Prof. Dr. D. S. Su
Shenyang National Laboratory for Materials Science
Institute of Metal Research, Chinese Academy of Science
72 Wenhua Road, Shenyang 110016 (China)

[**] This work was financially supported by the EnerChem project (Max Planck Society). D.S.S. is thankful for financial support of the 973 Program of China (Grant No. 2011CBA00504). B.F. wishes to acknowledge support by Dr. C. Bamberg.

Supporting information for this article is available on the WWW under <http://dx.doi.org/10.1002/anie.201006717>.

Table 1: Catalytic performance of nanocarbons.^[a]

| Catalyst | X [%] | | S [%] | | | | | Y(C ₄₌) [%] |
|----------|---------------------------------|---------------------------------|-------------------------------|----|-----------------|----|--|-------------------------|
| | 1-C ₄ H ₈ | 2-C ₄ H ₈ | C ₄ H ₆ | CO | CO ₂ | | | |
| SWCNT | 9 | 2 | 1 | 10 | 8 | 80 | | 1 |
| MWCNT | 12 | 3 | 1 | 16 | 8 | 72 | | 2 |
| UDD | 11 | 33 | 9 | 15 | 15 | 28 | | 6 |

[a] All data were collected after 10 h time-on-stream with stable catalytic performance (Figure 1 b).

network^[13] of *n*-butane ODH consisting of the target reaction and a consecutive reaction. Only 12 % selectivity for C₄ alkenes is observed for the single-walled carbon nanotubes (SWCNTs). 20 % selectivity for C₄ alkenes is obtained over the multi-walled carbon nanotubes (MWCNTs). For both CNT catalysts the concentration of butadiene is much higher than that of 1-butene and 2-butene. CO₂ is the predominant byproduct, whereas CO is only detected in trace amounts. Previous work showed that the oxidation of reactants and dehydrogenation products easily occurs on the nonmodified MWCNTs by nonquinoidic electrophilic oxygen species, thus resulting in a decrease in selectivity,^[4] this is also found to be the dominant process on SWCNTs.

UDD displays a superior catalytic performance. After 10 h time-on-stream (TOS), 11 % conversion and 56 % selectivity are observed. The concentrations of 1-butene and 2-butene are much higher than that of butadiene, hence suggesting that the further dehydrogenation is significantly hindered. A decrease in CO_x selectivity and an increase in the CO/CO₂ ratio points to the effective inhibition of *n*-butane combustion. Both effects complementarily indicate a reduced amount of electrophilic oxygen species, which 1) favor the unselective hydrocarbon oxidation and 2) are active in the oxidation of CO to CO₂^[14] (TPD profiles of fresh and used UDD: see Figure S1 in the Supporting Information). For the fresh catalyst, the desorption temperature of CO and CO₂ is around 850 K, respectively, thus indicating the presence of anhydride groups as the predominant oxygen species on the UDD surface. After reaction, both the CO and CO₂ desorption peaks shift to higher temperatures of 975 K and 925 K, respectively, which are assigned to quinone and lactone groups. The in situ removal of electrophilic oxygen functional groups and the generation of nucleophilic oxygen functional groups are related to the graphitization process. This result is consistent with our previous work and literature, thus confirming that the basic oxygen groups are the active sites for selective oxydehydrogenation. The comparison with used MWCNTs reveals that less oxygen groups are attached to the surface of UDD, hence indicating that not all of them are catalytically active. However, both the CO and CO₂ TPD profiles of MWCNTs have a noticeable low-temperature shoulder as a characteristic for acidic carboxyl and anhydride groups that act unselectively in the ODH. This observation is well reflected in the catalytic results shown in Table 1.

At the initial stage of catalytic testing, an increased *n*-butane conversion is observed (Figure 1 b). This observation might be attributed to initial *n*-butane adsorption on the catalyst surface as confirmed by the carbon balance around

95 % within the first 2 h TOS; however, the catalyst in its initial state is rather unselective for ODH, which is likely related to the poorly organized carbon overlayer that covers the crystalline UDD surface. A significant soot formation by hydrocarbon adsorption/decomposition can be excluded by stable BET surface areas of fresh and used samples. The superior catalytic performance arises within the first hours TOS and the highest selectivity is achieved after 2–3 h, where 11 % conversion and 60 % selectivity are observed. In the following, a slight decrease in selectivity is observed, associated with a weakly increasing *n*-butane conversion. The 100 h life testing of UDD (Figure 1 b) reveals that the catalyst reaches steady-state after 50 h TOS at around 13 % conversion and 47 % selectivity. The carbon balance is within 100 ± 1 % and the weight loss of the sample is negligible in comparison to other nanocarbons.^[15] Compared to the nanocarbons tested in previous^[4] and the present work, pristine UDD shows a significantly improved catalytic performance in the ODH of *n*-butane.

High-resolution TEM (HRTEM) reveals a diameter around 10–15 nm for the pristine UDD (Figure 2 a). The highlighted lattice fringes are identified as (111) planes of

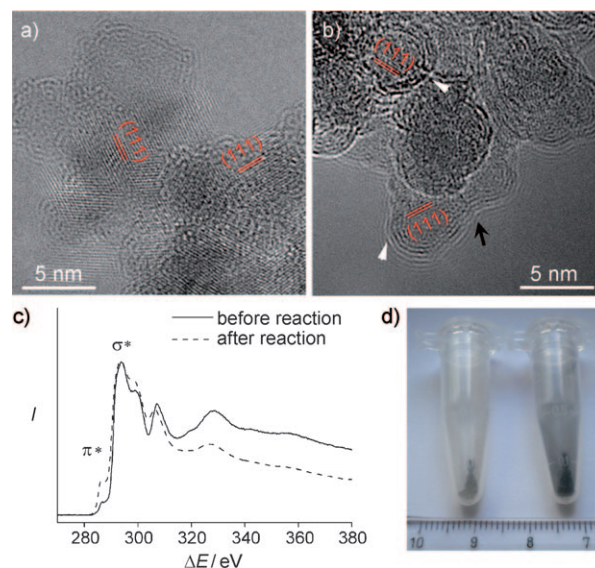


Figure 2. a) HRTEM image of pristine UDDs; b) HRTEM image of the catalyst sample after catalytic reaction; c) EELS profiles of nanocarbons before and after reaction; d) photographic illustration of catalysts before (left) and after (right) reaction.

diamond with an interplanar distance of 0.206 nm. Poorly organized carbon on the UDD surface is also observed; the dramatic change in morphology after reaction is demonstrated in Figure 2 b. Closed curved structures with concentric graphitic shells and diamond cores are observed (Figure 2 b, white arrows). The diameter of these structures ranges from 5–15 nm and consists of around 3–10 graphene layers, thus no significant change in size is observed. The formation of elongated particles with linked external graphitic layers and closed quasispherical internal shells was also observed, a so-called “peapod” geometry (black arrow).^[16] The graphitiza-

tion process was also identified by electron energy loss spectroscopy (EELS, Figure 2c). The main peaks > 290 eV were assigned to the three characteristic $1s-\sigma^*$ transitions, whereas the small peak at around 285 eV corresponds to the $1s-\pi^*$ transition assigned to graphitic carbon. A remarkable increase in $1s-\pi^*$ intensity was observed after catalytic reaction, thus proving the graphitization process induced by the catalytic test. Accordingly, the color of the catalyst changes from gray to black (Figure 2d).

The formation of fullerene shells can be attributed to the carbon redistribution of UDD because 1) the carbon balance during *n*-butane ODH is near 100 % and there is no change in weight during catalytic tests, which proves that the carbon deposition is negligible, 2) pristine UDD and obtained nanoparticles with core-shell microstructure provide the same size distribution, and 3) a radiation-induced transformation during HRTEM can be excluded since the samples were not exposed to an electron beam for a long time.^[17] Thus, the carbon source for the formation of fullerene shells comprises the graphitization of amorphous carbon deposit and carbon redistribution of nanodiamonds. This observation is finally supported by quantification based on the EELS spectra that indicate that the ratio of sp^2 carbon to sp^3 carbon rises from 10 to 25 % during the catalytic test.

The HRTEM images of UDD calcined at 773 K in an inert atmosphere (see the Supporting Information, Figure S2) prove that the thermal treatment at low temperature cannot induce the formation of onionlike shells. This observation is consistent with previous reports about similar core-shell nanocarbons or OLC synthesis by annealing of UDD (Table 2). The results suggest that the chemical adsorption

Table 2: Reaction conditions for phase transition from UDD to OLC.^[12]

| <i>d</i> [nm] | <i>T</i> ^[a] [K] | <i>T</i> ^[b] [K] | Environment | Products ^[c] | Ref. |
|---------------|-----------------------------|-----------------------------|------------------------|--------------------------|-------|
| 5 | 1273 | > 1423 | Ar, 1 bar | OLC shell + diamond core | [12a] |
| 5 | 1173 | > 1473 | 2 GPa | OLC, PHC, NR | [12b] |
| 5 | 1400 | 1900 | vacuum | OLC | [12c] |
| 5 | 1400 | 2140 | Ar | PHC, NR | [12c] |
| 5 | 1573 | 1873 | Ar, 1 bar | OLC, PHC, NR | [12d] |
| 5 | 773 | 1173 | O ₂ , 1 bar | combustion | [12d] |

[a] Onset temperature for graphitization; [b] temperature for complete conversion; [c] products found with complete conversion of UDD; PHC = polyhedral carbon nanoparticles, NR = nanoribbon, G = graphite.

and activation of hydrocarbon molecules and/or oxygen atoms on the surface of UDD is the ultimate factor for carbon redistribution. Consequently, it cannot be excluded that ppm traces of oxygen or water, which are likely present in the calcination experiments,^[12] are the key factors for the observed phase rearrangement. The similarity of the fresh and the calcined UDD was further confirmed by scanning electron microscopy (SEM, Figure 3). A strong charging effect is initially observed, caused by insulation of UDD (Figure 3a, arrows). Subsequently, the rapid aggregation (P) of nanoparticles by irradiation-induced surface graphitization

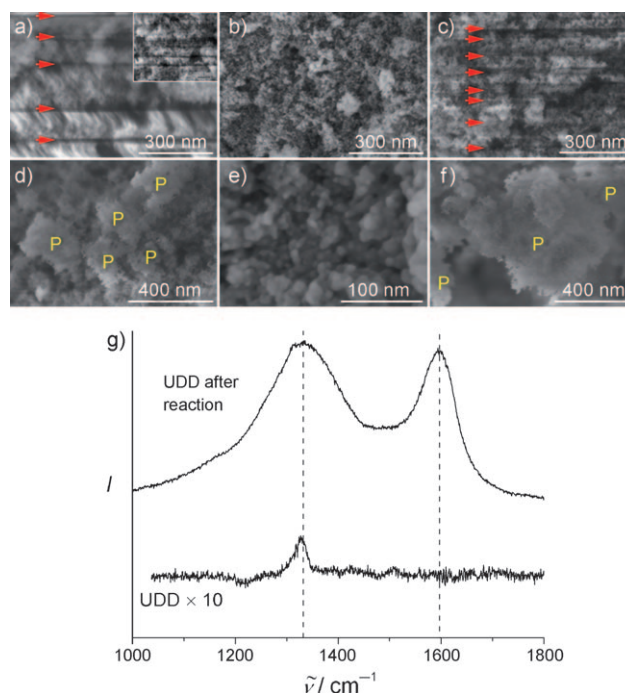


Figure 3. SEM images of a),d) pristine UDD, b),e) UDD after reaction, and c),f) calcined UDD. The inset in (a) is a low magnification SEM image. Red arrows indicate charging of the sample, whereas yellow Ps highlight the formed particles. g) Raman spectra of pristine and treated UDD samples.

occurs (Figure 3d).^[17] This phenomenon was also observed for the calcined UDD (Figure 3c and f), however, neither charging nor aggregation is observed for the UDD sample after reaction, which can be assigned to the formation of stable onionlike shells (Figure 3b,e).

Raman spectroscopy was applied to monitor the near-surface graphitization of the UDD sample during ODH catalysis (Figure 3g). After subtraction of the fluorescence background, the pristine material shows a tiny peak at 1330 cm^{-1} assigned to the diamond C–C bond with a long range order (F_{2g} mode). After reaction, two broad bands located at 1330 cm^{-1} and 1600 cm^{-1} appear, referred to as D (disordered) and G (graphitic) bands in carbon materials, respectively. Their appearance confirms the formation of nanocrystalline graphite clusters and the broad and intense D band points to a highly defective material as expected for the strongly curved OLC structure. Both the TEM and Raman analyses reveal that the OLC catalyst provides less amorphous carbon debris and surface defects compared to MWCNT catalysts used in the ODH of propane.^[5] Thus we conclude that the in situ transformation that gives rise to the active, selective, and stable surface is a straightforward requirement for the superior catalyst, as the amorphous carbon is known to favor combustion of hydrocarbons over their dehydrogenation.^[7]

The predominant influence of *n*-butane and oxygen has been identified on the chemically induced phase transition of ω -VOPO₄, and the effect is less pronounced with CO and H₂.^[9] It was hypothesized that the phase transition should be

related to oxygen vacancies and reduction of metal ions. However, the redistribution of UDD must follow a different mechanism wherein oxygen atom mobility was not taken into account. The mechanism of phase transition from UDD to OLC has been widely discussed. The C–C bonds between the outer and the subjacent (111) layers are reported to break and the outer layer consecutively flattens to form a dome-shaped strained graphitic seed.^[10,12c,18] Such induced formation of so-called “graphitic islands” is followed by pervasive graphitization. Exfoliated (111) planes of diamond link and tangle around the surface of the diamond particle, and then generate a closed graphene sheet. The inner diamond nanocrystal maintains its original shape and dwindles little by little in the course of transformation. As the consequence, a nanocarbon with onionlike shell and diamond core is formed.

Herein we present a promising member of the nanocarbon catalyst family that provides a high selectivity and stability in the ODH of *n*-butane. The superior nanocarbon catalyst with fullerene shell and diamond core is formed by the UDD precursor and the specific local environment, which is needed to embed the catalytically active sites, that is, the quinoidic carbonyl groups, is generated during the phase-transformation process from the sp^3 to the sp^2 hybridization state. The great difference in selectivities between CNTs and OLC implies that the well-graphitized surface strongly favors the selective alkane activation because of the controllable activation of oxygen. The strongly curved and strained graphitic surface that contains carbon atoms with a certain degree of sp^3 hybridization, appears to be an appropriate matrix for the selective generation of surface quinoidic groups and effectively suppresses the formation of electrophilic oxygen species such as carboxylic acids and their anhydrides. This assumption is supported by previous work, because P_2O_5 or B_2O_3 modification significantly decreases the total amount of oxidation.^[4,5,19] Changes in surface properties, for example heteroatom modification or carbon deposition, could be applied to improve the catalytic performance. High performance of such core-shell nanocarbon material has recently been demonstrated in the nonoxidative dehydrogenation of ethylbenzene to styrene.^[20] Similar to ODH type reactions, the surface redox couple of C=O and C–OH groups controls the catalytic turnover; however, the regeneration of the active site is achieved by oxidation of C–OH instead of thermal dehydrogenation.

Experimental Section

Catalytic tests were carried out in a quartz tubular reactor by using catalysts (180 mg) at 723 K and under atmospheric pressure. The total flow rate was 10 mL min^{−1} and the feed comprised 2.64 vol % *n*-butane and 1.32 vol % O₂ in He. Reaction products were quantified by gas chromatography (Varian 4900 Micro-GC). SWCNTs (SP7267) and MWCNTs (NC 3100) were obtained from Thomas Swan and Nanocyl, respectively. The thermal stability was tested by heating UDD (180 mg) at 773 K in a He flow of 10 mL min^{−1} for 90 h in the same fixed-bed reactor. Laser Raman spectroscopy was performed on powder samples by using an ISA LabRam instrument equipped with an Olympus BX40 microscope. The excitation wavelength was 632.8 nm and a spectral resolution of 0.9 cm^{−1} was used. HRTEM and EELS were performed using a Philips CM200 FEG transmission

electron microscope, operated at 200 kV. SEM images were obtained with a Hitachi S-4800 instrument, operated at 2 kV.

Received: October 26, 2010

Published online: March 1, 2011

Keywords: catalysis · nanodiamonds · nano-onions · phase transitions · surface activation

- [1] a) K. P. De Jong, J. W. Geus, *Catal. Rev. Sci. Eng.* **2000**, *42*, 481; b) P. Serp, J. L. Figueiredo, *Carbon Materials for Catalysis*, Wiley, Hoboken, **2009**; c) Inno.CNT—Innovationsallianz Carbon Nanotubes, <http://www.inno-cnt.de/> (accessed August 12, 2010); d) C. N. R. Rao, A. Sood, K. Subrahmanyam, A. Govindaraj, *Angew. Chem.* **2009**, *121*, 7890–7916; *Angew. Chem. Int. Ed.* **2009**, *48*, 7752–7777.
- [2] J. Zhang, D. S. Su, A. Zhang, D. Wang, R. Schlögl, C. Hébert, *Angew. Chem.* **2007**, *119*, 7460–7464; *Angew. Chem. Int. Ed.* **2007**, *46*, 7319–7323.
- [3] a) H. Xie, Z. Wu, S. H. Overbury, C. Liang, V. Schwartz, *J. Catal.* **2009**, *267*, 158–166; b) C. Liang, H. Xie, V. Schwartz, J. Howe, S. Dai, S. H. Overbury, *J. Am. Chem. Soc.* **2009**, *131*, 7735–7741; c) D. E. Resasco, *Nat. Nanotechnol.* **2008**, *3*, 708–709; d) D. S. Su, J. Zhang, B. Frank, A. Thomas, X. Wang, J. Paraknowitsch, R. Schlögl, *ChemSusChem* **2010**, *3*, 169–180; e) X. Wang, K. Maeda, A. Thomas, K. Takanabe, G. Xin, J. M. Carlsson, K. Domen, M. Antonietti, *Nat. Mater.* **2009**, *8*, 76–80; f) K. Chizari, I. Janowska, M. Houllé, I. Florea, O. Ersen, T. Romero, P. Bernhardt, M. J. Ledoux, C. Pham-Huu, *Appl. Catal. A* **2010**, *380*, 72–80.
- [4] J. Zhang, X. Liu, R. Blume, A. Zhang, R. Schlögl, D. S. Su, *Science* **2008**, *322*, 73–77.
- [5] B. Frank, J. Zhang, R. Blume, R. Schlögl, D. S. Su, *Angew. Chem.* **2009**, *121*, 7046–7051; *Angew. Chem. Int. Ed.* **2009**, *48*, 6913–6917.
- [6] J. P. Tessonier, A. Villa, O. Majoulet, D. S. Su, R. Schlögl, *Angew. Chem.* **2009**, *121*, 6665–6668; *Angew. Chem. Int. Ed.* **2009**, *48*, 6543–6546.
- [7] A. Rinaldi, J. Zhang, B. Frank, D. S. Su, S. B. Abd Hamid, R. Schlögl, *ChemSusChem* **2010**, *3*, 254–260.
- [8] a) J. Zhang, X. Wang, Q. Su, L. Zhi, A. Thomas, X. Feng, D. S. Su, R. Schlögl, K. Müllen, *J. Am. Chem. Soc.* **2009**, *131*, 11296–11297; b) M. F. R. Pereira, J. J. M. Órfão, J. L. Figueiredo, *Appl. Catal. A* **1999**, *184*, 153–160; c) Y. Iwasawa, H. Nobe, S. Ogasawara, *J. Catal.* **1973**, *31*, 444–449.
- [9] M. Conte, G. Budroni, J. K. Bartley, S. H. Taylor, A. F. Carley, A. Schmidt, D. M. Murphy, F. Girgsdies, T. Ressler, R. Schlögl et al., *Science* **2006**, *313*, 1270–1273.
- [10] V. L. Kuznetsov, A. L. Chuvilin, Y. V. Butenko, I. Y. Mal'kov, V. M. Titov, *Chem. Phys. Lett.* **1994**, *222*, 343–348.
- [11] N. R. Greiner, D. S. Phillips, J. D. Johnson, F. Volk, *Nature* **1988**, *333*, 440–442.
- [12] a) V. Kuznetsov, S. Moseenkov, A. Ischenko, A. Romanenko, T. Buryakov, O. Anikeeva, S. Maksimenko, P. Kuzhir, D. Bychanok, A. Gusinski et al., *Phys. Status Solidi B* **2008**, *245*, 2051–2054; b) J. Qian, C. Pantea, J. Huang, T. Zerda, Y. Zhao, *Carbon* **2004**, *42*, 2691–2697; c) V. L. Kuznetsov, Y. V. Butenko, V. I. Zaikovskii, A. L. Chuvilin, *Carbon* **2004**, *42*, 1057–1061; d) N. S. Xu, J. Chen, S. Z. Deng, *Diamond Relat. Mater.* **2002**, *11*, 249–256; e) O. Shenderova, C. Jones, V. Borjanovic, S. Hens, G. Cunningham, S. Moseenkov, V. Kuznetsov, G. McGuire, *Phys. Status Solidi A* **2008**, *205*, 2245–2251.
- [13] A. Wheeler, *Adv. Catal.* **1951**, *3*, 249–327.
- [14] A. Bielański, J. Haber, *Oxygen in Catalysis*, CRC, Boca Raton, FL, **1991**.

- [15] B. Frank, A. Rinaldi, R. Blume, R. Schlögl, D. S. Su, *Chem. Mater.* **2010**, 22, 4462–4470.
 - [16] R. Langlet, P. Lambin, A. Mayer, P. P. Kuzhir, S. A. Maksimenko, *Nanotechnology* **2008**, 19, 115706.
 - [17] V. V. Roddatis, V. L. Kuznetsov, Y. V. Butenko, D. S. Su, R. Schlögl, *Phys. Chem. Chem. Phys.* **2002**, 4, 1964–1967.
 - [18] A. Bródka, L. Hawelek, A. Burian, S. Tomita, V. Honkimäki, *J. Mol. Struct.* **2008**, 887, 34–40.
 - [19] B. Frank, M. Morassutto, R. Schomäcker, R. Schlögl, D. S. Su, *ChemCatChem* **2010**, 2, 644–648.
 - [20] J. Zhang, D. S. Su, R. Blume, R. Schlögl, R. Wang, X. Yang, A. Gajović, *Angew. Chem.* **2010**, 122, 8822–8826; *Angew. Chem. Int. Ed.* **2010**, 49, 8640–8644.
-